

Supporting Information

Bérut et al. 10.1073/pnas.1801895115

Methodology to Define and Fit the “Avalanche” and “Creep” Regimes

The avalanche and creep regimes discussed in the main text for statoliths (see Fig. 1 *C* and *D*) and silica particles (see Fig. 3 *C* and *D*) can be fitted by a linear function in a logarithmic time scale [$\theta = a \ln(t) + b$, where a and b are the two free parameters of the fit]. The critical angle θ_c between these two regimes can be initially estimated to be roughly $\theta_c \approx 10^\circ$.

Avalanche Regime. In the avalanche regime, the fit is done on all angles θ satisfying $\theta(t = 0) - \theta_{\text{thres}} \leq \theta \leq \theta_c + \theta_{\text{thres}}$, where θ_{thres} is an arbitrary threshold (chosen to avoid that θ is too close to the initial inclination angle and too close from θ_c where the regime is not well-defined). The characteristic time of the avalanche, t_a , is then defined as the time when the linear fit reaches $\theta = 0^\circ$ (see *Inset* of Fig. 1*C*). In the article, all values of t_a were computed with $\theta_{\text{thres}} = 5^\circ$. Fig. S1 shows that, for most of our measurements, t_a is independent of the choice of the threshold angle θ_{thres} .

Creep Regime. In the creep regime, the fit is done on all angles θ satisfying $\theta \leq \theta_c - \theta_{\text{thres}}$, where θ_{thres} is an arbitrary threshold. Good fits were obtained with $\theta_{\text{thres}} = 0^\circ$ for statolith avalanches and $\theta_{\text{thres}} = 5^\circ$ for the silica particle avalanches. The total avalanche duration, t_t , is defined as the time when the linear fit of the creep regime reaches an arbitrary small angle, taken as 2.5° in our paper (see Fig. 4*A*, *Inset*). For most data for which the pile angle actually reaches 2.5° during the experiment, the value of t_t only weakly depends upon the choice of θ_{thres} . By contrast, when the dynamic is so slow that the pile angle does not reach 2.5° before the end of the experiment (case of the $4.4 \mu\text{m}$ silica particles), the value of t_t can be very sensitive to the value of θ_{thres} . This explains why the error bars on the values of $\ln(t_t/t_a)$ in Fig. 4*A* are only visible for some points (for the other ones, the error bars are actually smaller than the size of the points themselves).

Finally, once the two regimes are fitted, one can verify that the value of the angle at the crossing point between them is close to the value of θ_c that was initially estimated. The obtained value over all our measurements is $\theta_c = 10.6^\circ$ (SD, 2.1°), which is in good agreement with our initial estimation of $\theta_c \approx 10^\circ$.

Statolith Avalanches for a Small Initial Inclination

Fig. 1*D*, *Inset* gives the time evolution of statolith piles for an initial inclination $\theta_i = 10^\circ$ below the critical angle, averaged

over six cells and for a given sample. To emphasize the convergence to horizontal of the pile angle despite the large fluctuations, we present in Fig. S2*A* the same data at different time windows before and after the inclination (orange symbols; the width of the window for averaging data are 30 s). We also show data for another experiment (blue symbols) that confirms the convergence to horizontal of weakly inclined piles. Interestingly, Fig. S2*B* shows that the temporal dynamics of relaxation for a small initial inclination ($\theta_i = 10^\circ$) is very similar to the long-time relaxation of piles with a large initial tilt ($\theta_i = 70^\circ$). This confirms that, in our microsystems, inertia can be neglected and the long-time “liquid-like” behavior is independent of the initial inclination.

Silica Particle Avalanches for a Small Initial Inclination

As shown in Fig. 1*D*, *Inset*, statolith piles relax to horizontal even when the initial inclination angle is very small (close to the value of θ_c). This phenomenon is also found for the silica particles, where the relaxation even occurs when the initial inclination angle is well below θ_c (see Fig. S3).

Dimensional Analysis

In the main text, we show experimentally that viscosity only changes the time scale of the silica particle avalanches but not the overall shape of the dynamics (the curves for two different viscosities collapse when time is rescaled by the viscosity; see Fig. 3*C*). Here we demonstrate that this behavior can be predicted by dimensional analysis when inertia is negligible, which is the case in our study. The time evolution of the pile angle θ for the silica particles depends on 11 parameters: t , θ_i , η , g , d , L , N , $\Delta\rho$, ρ , k , and T , where N is the number of particles in the pile and L the size of the pile (the other parameters are defined in the main text). These parameters have four dimensions (mass, length, time, and temperature). Dimensional analysis thus stipulates that θ should depend on $11 - 4 = 7$ dimensionless parameters—that is,

$$\theta = f(t\Delta\rho gL/\eta, Pe, \theta_i, N, d/L, \Delta\rho/\rho, Re), \quad (1)$$

where f is an unknown function and $Re = \rho(\Delta\rho gL^2/\eta)L/\eta$ is the Reynolds number. In our study, the dependence of the function f with the Reynolds number can be neglected because inertia is negligible (Reynolds numbers are always below 10^{-3}). Therefore, the fluid viscosity η only appears as a scale factor of the time t in Eq. 1.

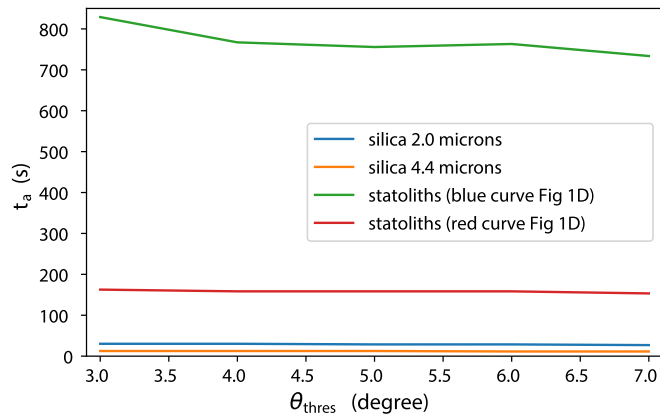


Fig. S1. Characteristic time of the avalanche t_a , computed for several values of the threshold angle θ_{thres} . For silica particles, the value of t_a was always found between 10 s and 30 s; for the statoliths, the value of t_a can vary between 150 s and 850 s depending on the sample.

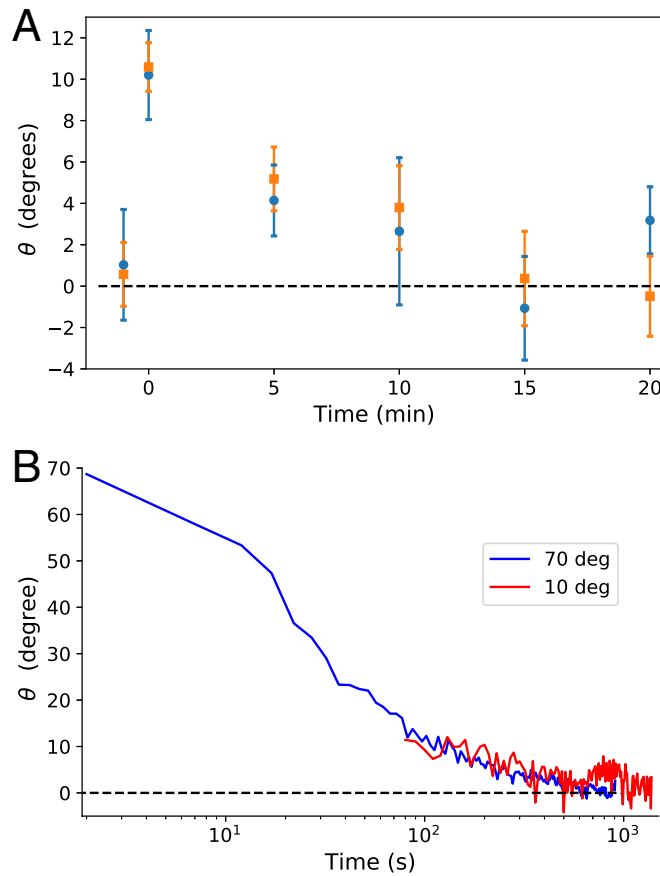


Fig. S2. Statolith avalanches at small inclination angles. (A) Statolith pile angle before and after inclination for an initial inclination $\theta_i = 10^\circ$ (at $t = 0$), at discrete time intervals, for two different samples. Data are averaged over a time window of 30 s. The vertical error bars give the SD between the n different cells of each symbol ($n = 6$ and $n = 8$). (B) Superposition of the statolith dynamics for an initial inclination $\theta_i = 70^\circ$ (blue) and $\theta_i = 10^\circ$ (red) (data corresponding to Fig. 1 C and D, *Inset*). The red curve has been shifted in time for matching the blue curve at 10° .

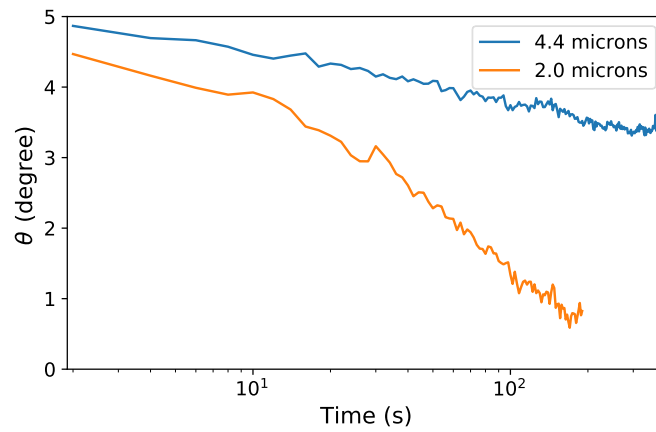
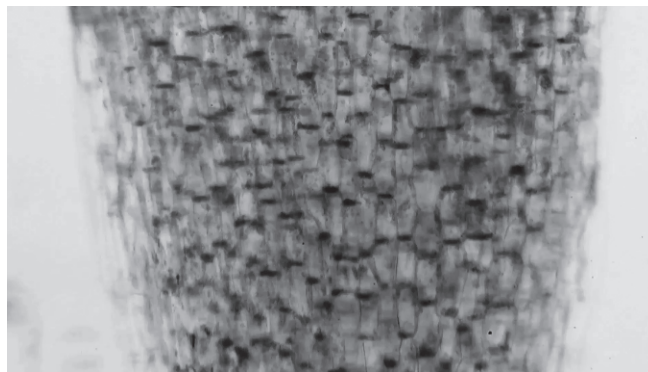
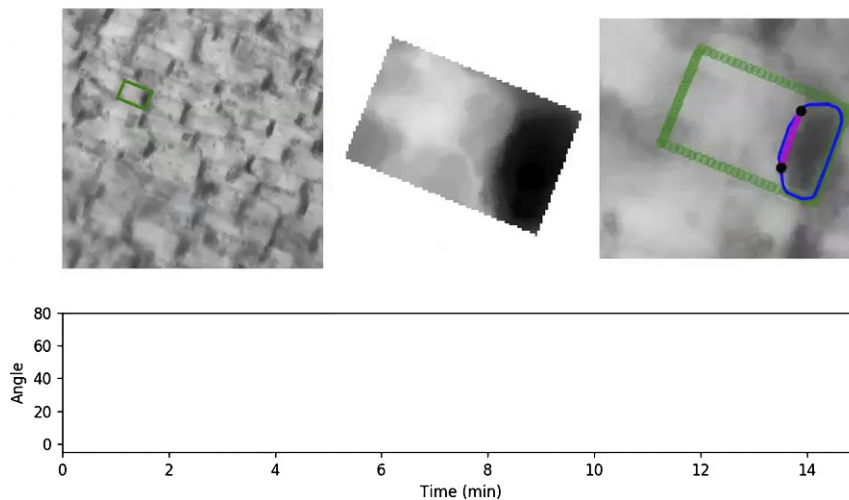


Fig. S3. Avalanches of silica particles (4.4 μm and 2.0 μm) for an initial inclination angle $\theta_i = 5^\circ < \theta_c$ (averaged over $n = 41$ and $n = 43$ biomimetic cells). For both particle sizes, the pile shows relaxation toward the flat angle, but the dynamic is much more slower for bigger (i.e., less agitated) particles.



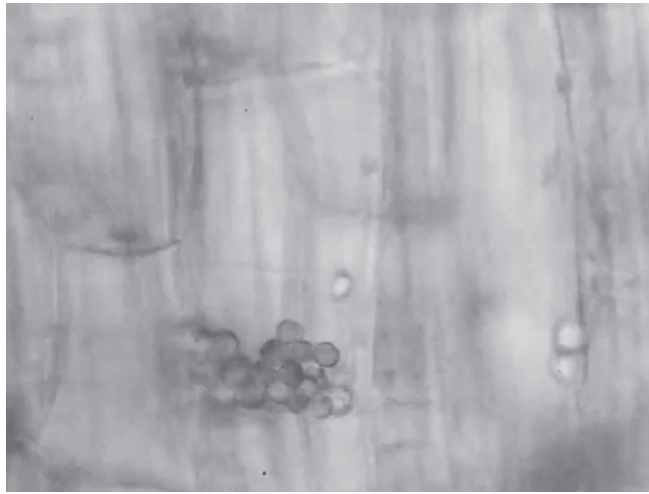
Movie S1. Wide view of statolith avalanches in a wheat coleoptile cut in bright field after an initial tilt of the cells $\theta_i = 70^\circ$ (objective $10\times$). Each dark spot corresponds to a pile of statoliths. The movie is accelerated $40\times$; the real duration of the movie is about 10 min (real time between successive images is 1.7 s).

[Movie S1](#)



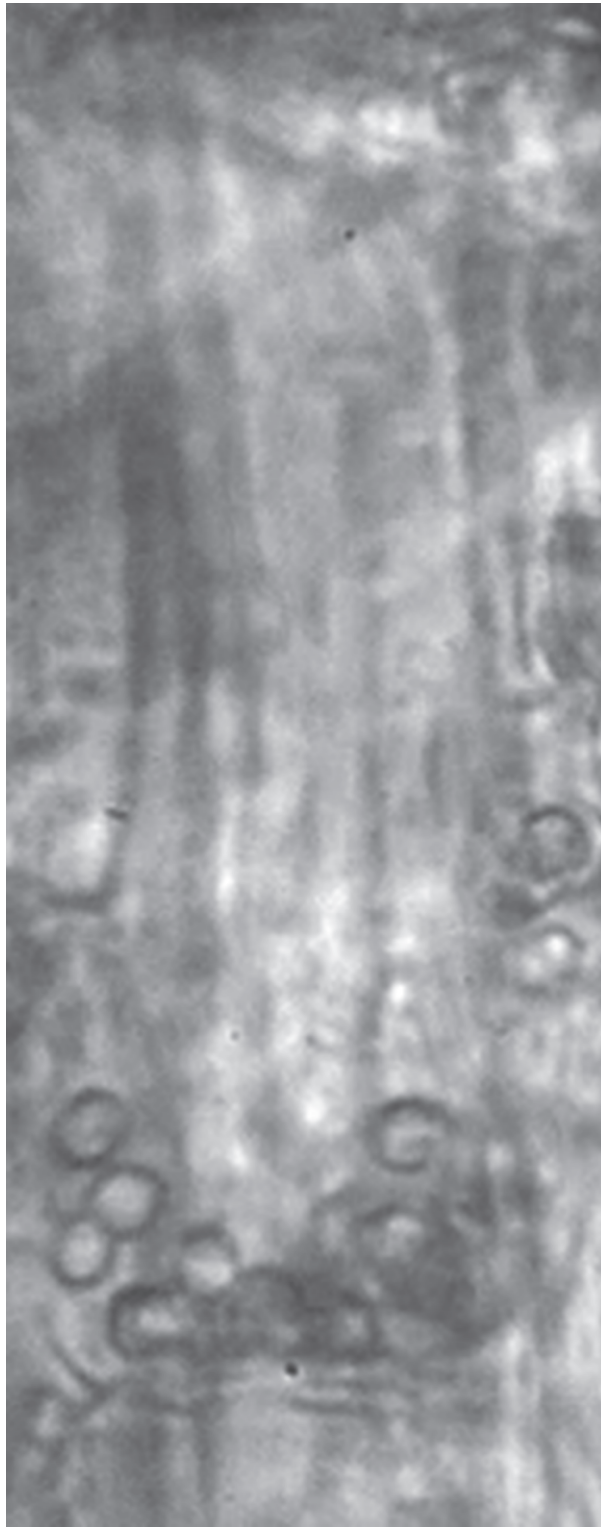
Movie S2. Detection technique of the free surface of the statolith piles during an avalanche with the corresponding pile angle versus time. The movie is accelerated $120\times$; the real duration of the movie is about 14 min (real time between successive images is 5 s).

[Movie S2](#)



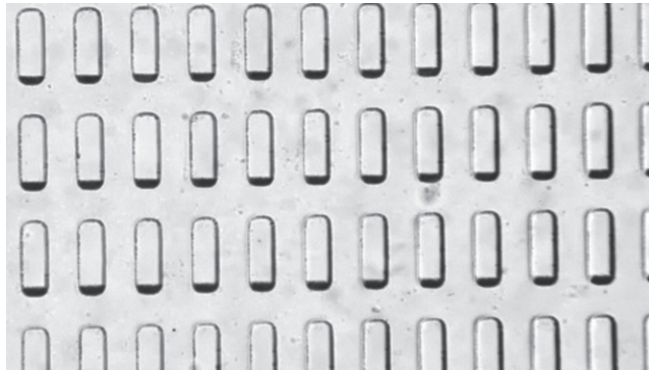
Movie S3. Close-up view of a statolith avalanche after an initial tilt $\theta_i = 15^\circ$, showing the fluctuation motion of statoliths (objective 40 \times). The movie is accelerated 80 \times ; the real duration of the movie is 857 s (real time between successive images is 3.3 s).

[Movie S3](#)



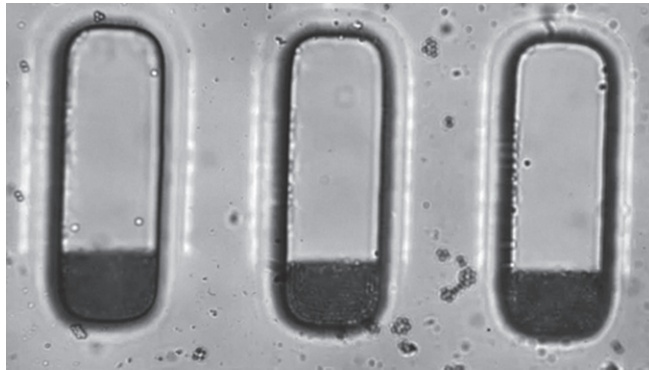
Movie S4. Close-up view of statolith fluctuation in a cell at rest under gravity (objective 40 \times). The movie is accelerated 10 \times ; the real duration of the movie is 4 min (real time between successive images is 0.42 s).

[Movie S4](#)



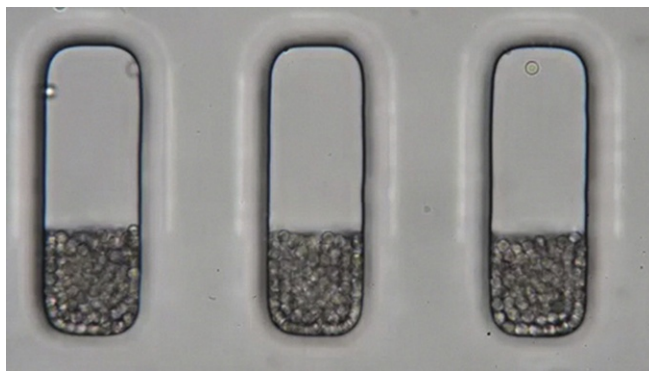
Movie S5. Wide view of "statolikes" avalanches in biomimetic cells (silica particles $2\ \mu\text{m}$ in diameter immersed in water) after an initial tilt $\theta_i = 70^\circ$ (objective $10\times$). The movie is accelerated $10\times$; the real duration of the movie is 2 min (real time between successive images is 0.42 s).

[Movie S5](#)



Movie S6. Close-up on avalanches of $2\ \mu\text{m}$ silica particles after an initial tilt $\theta_i = 20^\circ$, showing liquid-like relaxation to horizontal (objective $40\times$). The movie is accelerated $10\times$; the real duration of the movie is 2 min (real time between successive images is 0.42 s).

[Movie S6](#)



Movie S7. Close-up on avalanches of $4.4\ \mu\text{m}$ silica particles after an initial tilt $\theta_i = 10^\circ$, showing almost no relaxation below the critical angle, like a granular material (objective $40\times$). The movie is accelerated $10\times$; the real duration of the movie is 2 min (real time between successive images is 0.42 s).

[Movie S7](#)